LUND UNIVERSITY

Car-to-car radio channel measurements at 5 GHz: Pathloss, power-delay profile, and delay-Doppler spectrum

Paier, Alexander; Kåredal, Johan; Czink, Nicolai; Hofstetter, Helmut; Dumard, Charlotte; Zemen, Thomas; Tufvesson, Fredrik; Molisch, Andreas; Mecklenbräuker, Christoph

Published in:
[Host publication title missing]

DOI:
10.1109/ISWCS.2007.4392335

2007

Link to publication

Citation for published version (APA):
Paier, A., Kåredal, J., Czink, N., Hofstetter, H., Dumard, C., Zemen, T., Tufvesson, F., Molisch, A., & Mecklenbräuker, C. (2007). Car-to-car radio channel measurements at 5 GHz: Pathloss, power-delay profile, and delay-Doppler spectrum. In *[Host publication title missing]* (pp. 224-228). IEEE - Institute of Electrical and Electronics Engineers Inc.. https://doi.org/10.1109/ISWCS.2007.4392335

Total number of authors:
9

General rights
Unless other specific re-use rights are stated the following general rights apply:
Copyright and moral rights for the publications made accessible in the public portal are retained by the authors and/or other copyright owners and it is a condition of accessing publications that users recognise and abide by the legal requirements associated with these rights.
• Users may download and print one copy of any publication from the public portal for the purpose of private study or research.
• You may not further distribute the material or use it for any profit-making activity or commercial gain
• You may freely distribute the URL identifying the publication in the public portal

Read more about Creative commons licenses: https://creativecommons.org/licenses/

Take down policy
If you believe that this document breaches copyright please contact us providing details, and we will remove access to the work immediately and investigate your claim.

LUND UNIVERSITY

PO Box 117
221 00 Lund
+46 46-222 00 00

Download date: 19. Apr. 2024

Car-to-car radio channel measurements at 5 GHz: Pathloss, power-delay profile, and delay-Doppler spectrum

Alexander Paier[1], Johan Karedal[4], Nicolai Czink[1,2], Helmut Hofstetter[3], Charlotte Dumard[2], Thomas Zemen[2], Fredrik Tufvesson[4], Andreas F. Molisch[4,5], Christoph F. Mecklenbräuker[1]

[1]Institut für Nachrichtentechnik und Hochfrequenztechnik, Technische Universität Wien, Vienna, Austria
[2]Forschungszentrum Telekommunikation Wien (ftw.), Vienna, Austria
[3]mobilkom austria AG, Vienna, Austria
[4]Department of Electrical and Information Technology, Lund University, Lund, Sweden
[5]Mitsubishi Electric Research Labs, Cambridge, USA
Contact: apaier@nt.tuwien.ac.at

***Abstract*— We carried out a car–to–infrastructure (C2I) and car–to–car (C2C) 4×4 multiple–input multiple–output (MIMO) radio channel measurement campaign at 5.2 GHz in Lund, Sweden. This paper presents first results on pathloss, power–delay profiles, and delay–Doppler spectra in a C2C highway scenario, where both cars were traveling in opposite directions. A pathloss coefficient of 1.8 yields the best fit with our measurement results in the mean square sense. The measured Doppler shift of the line of sight path matches exactly with theoretical calculations. Selected paths are investigated in the delay and Doppler domain. The averege delay spread is 250 ns; Doppler shifts of more than 1000 Hz are observed.**

I. Introduction

A novel wireless local area network technology for car–to–car and –infrastructure communications (in the following summarized as "C2X") is being drafted by IEEE task group 802.11p [1]. Many aspects of the C2X radio channel in the 5 GHz band are yet to be understood, e.g. the statistics of time–selective fading.

Earlier C2X measurements report exclusively on the car–to–car (C2C) case with cars driving in the *same* direction [2], [3], [4], [5]. However, we show in this contribution that C2C with cars traveling in *opposite* directions and car–to–infrastructure (C2I), results in much higher Doppler shifts. In [2], [3], the radio channel is investigated at 2.4 GHz, and [5] presents a narrow–band measurement campaign. Measured and simulated Doppler spectra for a frequency selective C2I channel are reported in [6]. C2I MIMO pathloss measurements are presented in [7].

In order to alleviate the current lack of measurement data, we carried out a C2X radio channel measurement campaign in the 5 GHz band in Lund, Sweden. A detailed description of the measurement setup, and preliminary results for urban environments, can be found in [8]. In this paper, we focus on the evaluation of pathloss, power–delay profile, and delay–Doppler spectrum in a highway scenario.

II. Measurements

A. Measurement equipment

As measurement cars we used two transporters (similar to pickup trucks), of the same type, see Fig. 1. The measurements were carried out with the RUSK LUND channel sounder which is based on the "switched–array" principle [9]. The measurement setup of the RUSK LUND channel sounder is summarized in Tab. I. The snapshot repetition rate is $t_{\text{rep}} = 307.2\,\mu$s. With these settings, the maximum resolvable Doppler shift is 1.6 kHz corresponding to a maximum speed of 94 m/s (338 km/h). From the channel transfer functions acquired by the channel sounder, we obtain the complex channel impulse responses (IRs) by an inverse Fourier transform using the Hanning window, giving $h(nt_{\text{rep}}, k\Delta\tau, p)$. These IRs are stored in an array of size $N \times K \times P$ with $N = 32500$, $K = 769$, and $P = 16$. Here, n is the time index, from $n = 0, \ldots, N-1$, k is the delay index, $k = 0, \ldots, K-1$, and p is the channel number, $p = 1, \ldots, P$. A more detailed description of the measurement equipment and practice can be found in [8].

B. Measurement scenario

In this paper we present evaluation results from a selected highway C2C measurement run, where the cars were traveling in opposite directions. Each car was traveling with a speed of 90 km/h, which results in a relative speed of 180 km/h between the two cars. There was medium traffic on the highway. Fig. 1 shows a photo before the cars were passing, taken from the Tx car's passenger compartment. Fig. 2 shows a satellite photo of the highway scenario. As indicated in this figure the Tx car was heading southwestward and the Rx car northeastward. In the considered 10 s measurement run the two cars were passing after 7.5 s.

Authorized licensed use limited to: IEEE Xplore. Downloaded on January 30, 2009 at 07:01 from IEEE Xplore. Restrictions apply.

TABLE I

MEASUREMENT PARAMETERS

Center frequency, f	5.2 GHz
Measurement bandwidth, BW	240 MHz
Delay resolution, $\Delta\tau = 1/BW$	4.17 ns
Transmit power, P_{Tx}	27 dBm
Test signal length, $\tau_{\max}$	3.2 μs
Number of Tx antenna elements, N_{Tx}	4
Number of Rx antenna elements, N_{Rx}	4
Snapshot time, t_{snap}	102.4 μs
Snapshot repetition rate, t_{rep}	307.2 μs
Number of snapshots, N	32500
Recording time, t_{rec}	10 s
File size, FS	1 GB
Tx antenna height, h_{Tx}	2.4 m
Rx antenna height, h_{Rx}	2.4 m

Fig. 1. Photo of the highway from the passenger compartment

Fig. 2. Satellite photo of the highway E22 in the east of Lund

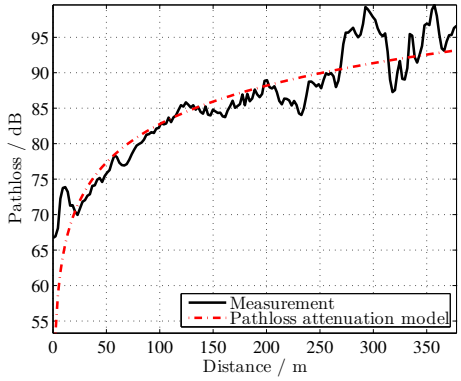

Fig. 3. Comparison between measured pathloss and pathloss calculated with pathloss model with exponent 1.8

III. EVALUATION RESULTS

A. Pathloss

For calculation of the pathloss the receive power is calculated by averaging the magnitude squared over 40 wavelengths, in order to average over the small scale fading, and taking the sum over the delay domain and all 16 channels

$$P_{\mathrm{Rx}}(it_{\mathrm{av}}) = \frac{1}{L} \sum_{n=iL}^{(i+1)L-1} \sum_{k=0}^{K-1} \sum_{p=1}^{P} |h(nt_{\mathrm{rep}}, k\Delta\tau, p)|^2. \quad (1)$$

Forty wavelengths are equal to 2.3 m and thus yield at a relative speed of 180 km/h an averaging time of $t_{\mathrm{av}} = 46$ ms, i.e. $L = 150$ snapshots. Before summing up the power in the delay domain, we use a noise threshold of 60 dB below the maximum. All values below this threshold are considered as noise and therefore set to zero. The pathloss is calculated by taking the difference of the transmit power of 27 dBm and the receive power in logarithmic scale. Figure 3 compares this pathloss with the result of a calculation with the pathloss attenuation model with an exponent of 1.8. This exponent yields the lowest root mean square (RMS) error of 3.3 dB. The measurement results are taken from the first 7.5 s of our measurement run, where the two cars were approaching each other.

B. Power–delay profile

Similar to the calculation of the receive power we calculate the short–time average power–delay profile (PDP) by averaging the magnitude squared over 40 wavelengths, $L = 150$ snapshots, and taking the sum over all $P = 16$ antenna–to–antenna channels

$$P_{\mathrm{PDP}}(it_{\mathrm{av}}, k\Delta\tau) = \frac{1}{L} \sum_{n=iL}^{(i+1)L-1} \sum_{p=1}^{P} |h(nt_{\mathrm{rep}}, k\Delta\tau, p)|^2. \quad (2)$$

Figure 4 (a) shows the strong line of sight (LOS) path with decreasing delay until 7.5 s (cars passing) and increasing delay afterwards. There are also several paths that are approximately parallel to the LOS path. These paths result from reflections from cars, which are traveling with approximately the same speed as our measurement cars. Such a path is exactly parallel to the LOS path iff the speed of the reflecting car and the measurement car is equal. Further there is a group of paths from approximately 5 s to 10 s, which are slightly decreasing from a delay of about 700 ns to 600 ns until a time of 7.5 s and increasing afterwards. These paths are much stronger than most of the paths, which are parallel to the LOS path. The

Authorized licensed use limited to: IEEE Xplore. Downloaded on January 30, 2009 at 07:01 from IEEE Xplore. Restrictions apply.

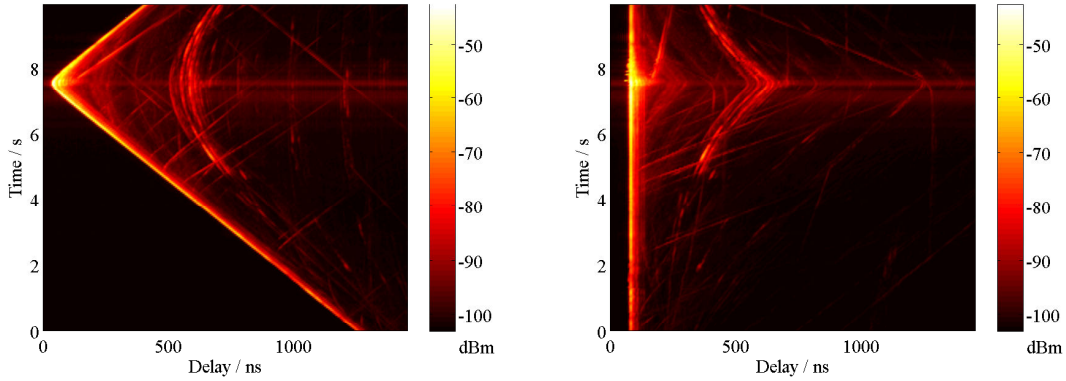

Fig. 4. (a) Average power–delay profile, (b) average power–delay profile with shifted LOS paths to delay 83 ns

most likely explanation for this group of paths is scattering at factory buildings in the southeast of the highway, see Fig. 2. Note that such paths should show a Doppler shift that is less than the Doppler shift of the LOS path, because the angle between driving direction and wave propagation direction is larger than zero. We will show this in Sec. III-C.

In Fig. 4 (b) the maximum of the LOS path is shifted to a constant delay of 83 ns. These shifted paths are also used for all further calculations of the PDPs and delay–Doppler spectra in this paper. As a result of this shifting, the paths resulting from reflections at other cars are not anymore parallel to the LOS path.

The average mean excess delay as defined in [10],

$$\bar{\tau}(it_{\mathrm{av}}) = \sum_{k=0}^{K-1} k\Delta\tau P_{\mathrm{PDP}}(it_{\mathrm{av}}, k\Delta\tau) \Big/ P_{\mathrm{Rx}}(it_{\mathrm{av}})$$

is approximately 52 ns. For this calculation the peak of the LOS path is shifted to delay zero and we use a threshold of 60 dB below the maximum. The root mean square (RMS) delay spread is the square root of the second central moment of the PDP, [10]. Similar to the calculation of mean excess delay the noise threshold is set to 60 dB below the maximum. The average RMS delay spread over all snapshots

$$\tau_{\mathrm{rms}}(it_{\mathrm{av}}) = \sqrt{\sum_{k=0}^{K-1} (k\Delta\tau - \bar{\tau}(it_{\mathrm{av}}))^2 P_{\mathrm{PDP}}(it_{\mathrm{av}}, k\Delta\tau) \Big/ P_{\mathrm{Rx}}(it_{\mathrm{av}})}$$

is approximately 247 ns and its cumulative distribution function (CDF) is shown in Fig. 5.

Beside the short–time PDP we also define a long–time PDP which is averaged over 0.5 s. In the case of a relative speed of 180 km/h the two cars travel 25 m in 0.5 s. For this long–time PDP we use Eq. (2) with $L = 1800$ instead of $L = 150$. Figure 6 shows the long–time PDP from snapshot 16200 to 17999 which is equal to a time from 5 s to 5.5 s. The LOS path is shifted to delay 83 ns. The second strongest path at 371 ns is the one scattered at factory buildings, described above. The difference in propagation delay between this path and the LOS path is 288 ns corresponding to 86 m.

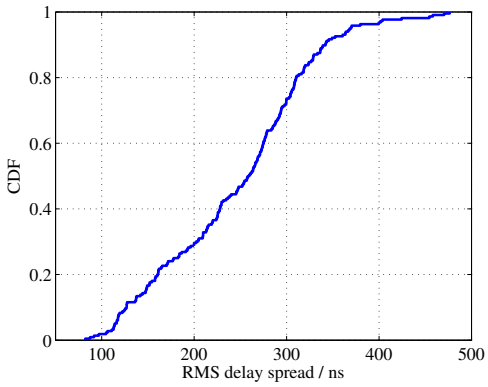

Fig. 5. CDF of RMS delay spread with threshold of 60 dB below maximum

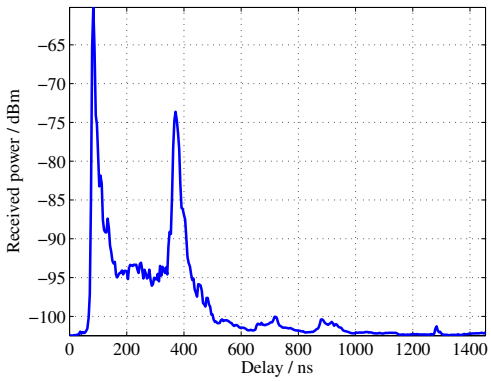

Fig. 6. Long–time average PDP at 5 s

Six short–time PDPs, each over a duration of 46 ms, from 5 s to 5.5 s are depicted in Fig. 7. This is the same time period as for the long–time PDP in Fig. 6. There are some changes of the short–time PDP over this time period. On the left side at delay 83 ns the LOS path is constant over this 0.5 s, which is a consequence of shifting this path to this delay. After the LOS path, there is a small peak, starting at a delay of 133 ns at the first short–time PDP at 5 s. The delay of this peak is

Authorized licensed use limited to: IEEE Xplore. Downloaded on January 30, 2009 at 07:01 from IEEE Xplore. Restrictions apply.

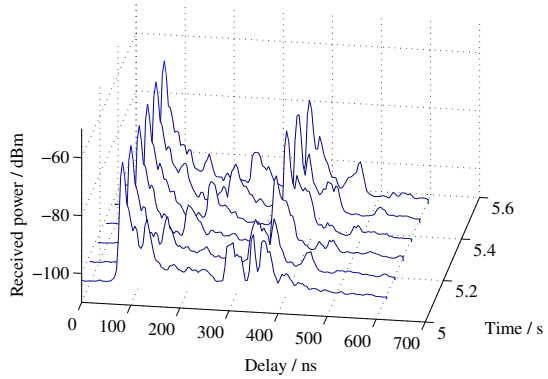

Fig. 7. Short–time average PDPs from 5 s to 5.5 s

increasing until the last PDP, at 5.5 s, to 275 ns. Also the peak at approximately 370 ns, which is the path described above in Fig. 6, is changing from the first short–time PDP with three small peaks to one large peak and a second smaller peak in the last PDP. This shows the non–stationarity of the radio channel over the time period of 0.5 s.

C. Delay–Doppler spectrum

At first the LOS path is shifted to the delay 83 ns as described in the last section. We calculate the delay–Doppler spectrum

$$P_{\mathrm{DD}}(r\Delta\nu, k\Delta\tau) = \sum_{p=1}^{P} |f_{\mathrm{fft}}(h(nt_{\mathrm{rep}}, k\Delta\tau, p))|^2, \qquad (3)$$

using the fast–Fourier transformation (FFT) from Matlab and taking the sum of the magnitude squared over all 16 channels. For the short–time delay–Doppler spectrum we perform the FFT over 150 snapshots which results in a Doppler resolution of $\Delta\nu = 22\,\mathrm{Hz}$, for $-75 \leq r \leq 74$, and for the long–time delay–Doppler spectrum over 1800 snapshots which results in a higher resolution of $\Delta\nu = 2\,\mathrm{Hz}$, for $-900 \leq r \leq 899$.

Fig. 8 (a) and (b) show the short–time and long–time logarithmic normalized delay–Doppler spectra

$$P_{\mathrm{DD,norm}}(r\Delta\nu, k\Delta\tau) = \frac{P_{\mathrm{DD}}(r\Delta\nu, k\Delta\tau)}{\max(P_{\mathrm{DD}}(r\Delta\nu, k\Delta\tau))}, \qquad (4)$$

after a time of 5 s of the measurement run, respectively. In the following we describe peaks with their maxima at (i) 83 ns / 868 Hz, (ii) 371 ns / 543 Hz, and (iii) 304 ns / −1107 Hz. Peak (i) is the LOS path with a Doppler shift of 868 Hz, corresponding to a relative speed of 180 km/h between Tx and Rx, which agrees exactly with the intended speed. Positive Doppler frequencies indicate that the cars are approaching. Peak (ii) is the path scattered at the factory buildings with a Doppler shift of 543 Hz, see Fig. 9. Note that this Doppler shift, which is between zero and the LOS Doppler shift, is congruent with our deductions in Sec. III-B. Considering the delay of peak (iii) we can find in Fig. 4 that it is approximately parallel to the LOS path delay. With a Doppler shift of −1107 Hz this path comes from a reflection from a car, with a

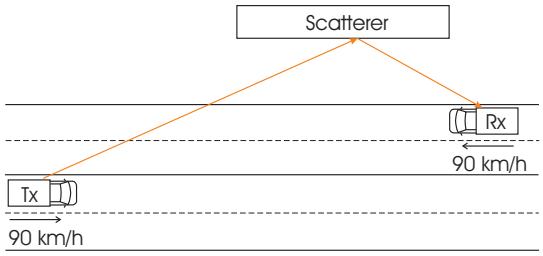

Fig. 9. Doppler shift scenario (ii)

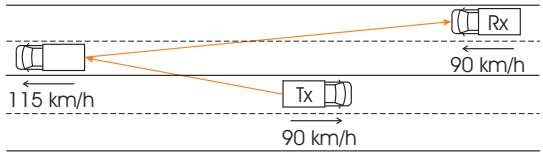

Fig. 10. Doppler shift scenario (iii)

speed of 115 km/h, 25 km/h faster than the measurement cars. Figure 10 depicts this scenario. The long–time delay–Doppler spectrum in Fig. 8 (b) displays roughly the same peaks, but much more blurred, because of the delay varying over time. In combination with the short–time delay–Doppler spectrum the delay variation over time can be observed.

D. Doppler shift of LOS path

In this section we compare the theoretically calculated Doppler shift of the LOS path

$$\nu(t) = -\frac{v}{\lambda}\cos(\gamma(t)), \qquad (5)$$

where $v = 180\,\mathrm{km/h}$ is the relative speed between the two cars, $\lambda = 58\,\mathrm{mm}$ is the wavelength, and $\gamma(t)$ is the angle between driving direction and LOS path direction, with the measured Doppler shift of this path. The LOS Doppler shift of the measurement run is calculated as described in Sec. III-C. After shifting the LOS path to a constant delay in the time domain we calculate the short–time delay–Doppler spectrum with Eq. (3). This is done for the whole 10 s measurement run with equidistant snapshot periods of 150, for short–time delay–Doppler spectrum. The Doppler shift is extracted, by taking the maximum of each of this 150 snapshot periods at the fixed delay of 83 ns in the Doppler domain.

Figure 11 shows the range between the two cars in the upper figure and the calculated and measured Doppler shift in the figure below. The range of the cars when they passed each other was not zero, but 10 m, which equals to the width of two lanes plus the space between two opposite lanes. The measured Doppler shift (black crosses) and the calculated Doppler shift (blue curve) fit very well.

IV. Conclusions

In this paper results from car–to–car (C2C) measurements at 5.2 GHz are presented. One of the great advantages of these measurements is the high measurement bandwidth of 240 MHz and the high Doppler sampling rate which allows a

Authorized licensed use limited to: IEEE Xplore. Downloaded on January 30, 2009 at 07:01 from IEEE Xplore. Restrictions apply.

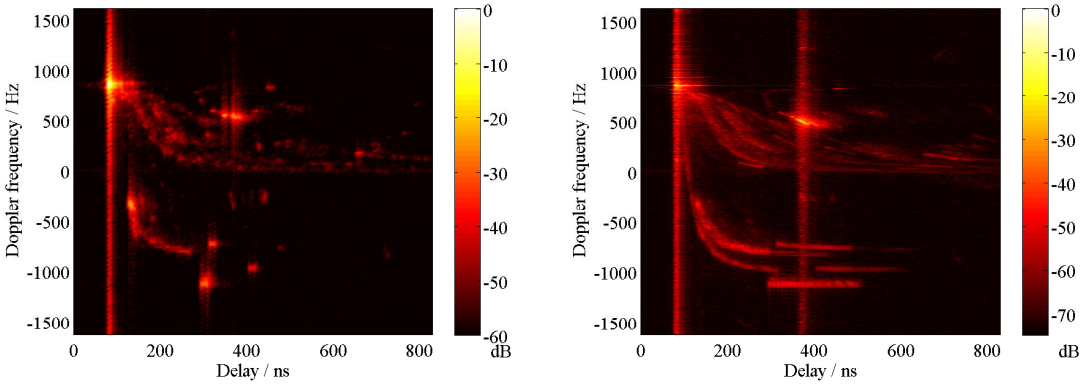

Fig. 8. (a) Short–time delay–Doppler spectrum at 5 s (time window of 43 ms), (b) long–time delay–Doppler spectrum at 5 s (time window of 0.5 s)

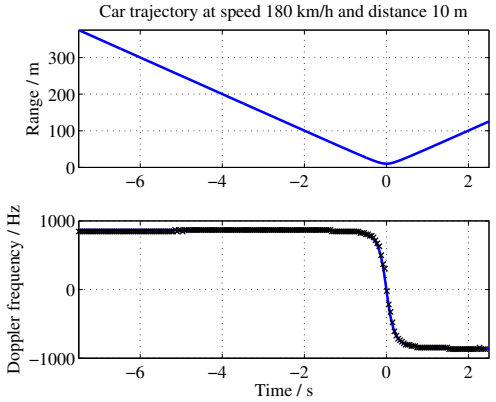

Fig. 11. Comparison of measured and calculated Doppler shift of the LOS path

maximum Doppler shift of 1.6 kHz in a 4×4 MIMO system. The measurements were carried out in Lund, Sweden. The paper presents results of evaluating C2C channels, in a typical highway scenario, with the cars driving in opposite directions, each with 90 km/h.

By comparing the measured pathloss with the pathloss attenuation model we found that an attenuation exponent of 1.8 yields the lowest root mean square (RMS) error of 3 dB. We found an average mean excess delay of 52 ns and an average RMS delay spread of 247 ns. The line of sight (LOS) path shows exactly the theoretically calculated Doppler shift at a relative speed of 180 km/h. Beside this strong LOS path, we observe several paths approximately parallel to this path, which were reflected at other cars on the highway. Other strong paths were found, scattering at factory buildings beside the highway. These paths have a Doppler shift less than the Doppler shift of the LOS path, which agrees with the theory of the Doppler shift, when the angle between driving direction and wave propagation direction is not equal to zero.

After these promising first results, we will further analyze the measurements in order to characterize the three different scenarios, rural, highway, and typical–Lund–urban, and especially the dependence of the results on the different antenna elements.

V. Acknowledgements

We would like to thank RIEGL Laser Measurement Systems GmbH and MEDAV GmbH for their generous support. This work was carried out with partial funding from Kplus and WWTF in the ftw. projects I0 and I2 and partially by an INGVAR grant of the Swedish Strategic Research Foundation (SSF), and the SSF Center of Excellence for High–Speed Wireless Communications (HSWC).

References

[1] "Draft amendment to wireless LAN medium access control (MAC) and physical layer (PHY) specifications: Wireless access in vehicular environments," IEEE P802.11p^{tm}/D2.01, March 2007.

[2] G. Acosta, K. Tokuda, and M. A. Ingram, "Measured joint doppler-delay power profiles for vehicle-to-vehicle communications at 2.4 GHz," in *Global Telecommunications Conference 2004*, 29 November – 3 December 2004.

[3] G. Acosta and M. A. Ingram, "Model development for the wideband expressway vehicle-to-vehicle 2.4 GHz channel," in *IEEE Wireless Communications and Networking Conference (WCNC) 2006*, 3–6 April 2006.

[4] G. Acosta-Marum and M. A. Ingram, "Doubly selective vehicle-to-vehicle channel measurements and modeling at 5.9 GHz," in *Wireless Personal Multimedia Communications (WPMC) 2006*, 17–20 September 2006.

[5] J. Maurer, T. Fügen, and W. Wiesbeck, "Narrow-band measurement and analysis of the inter-vehicle transmission channel at 5.2 GHz," in *Vehicular Technology Conference (VTC) 2002*, 6–9 May 2002.

[6] X. Zhao, J. Kivinen, P. Vainikainen, and K. Skog, "Characterization of doppler spectra for mobile communications at 5.3 GHz," in *IEEE Transaction on Vehicular Technology*, January 2003.

[7] C. Schneider, A. Hong, G. Sommerkorn, M. Milojevic, and R. S. Thomä, "Path loss and wideband channel model parameters for WINNER link and system level evaluation," in *Third International Symposium on Wireless Communication Systems (ISWCS) 2006*, 5–8 September 2006.

[8] A. Paier, J. Karedal, N. Czink, H. Hofstetter, C. Dumard, T. Zemen, F. Tufvesson, A. F. Molisch, and C. F. Mecklenbräuker, "First results from car-to-car and car-to-infrastructure radio channel measurements at 5.2 GHz," in *International Symposium on Personal, Indoor and Mobile Radio Communications (PIMRC) 2007*, September 2007.

[9] R. Thomä, D. Hampicke, A. Richter, G. Sommerkorn, A. Schneider, U. Trautwein, and W. Wirnitzer, "Identification of time-variant directional mobile radio channels," *IEEE Trans. on Instrumentation and measurement*, vol. 49, pp. 357–364, 2000.

[10] A. F. Molisch, *Wireless Communications*. John Wiley and Sons, 2005.

Authorized licensed use limited to: IEEE Xplore. Downloaded on January 30, 2009 at 07:01 from IEEE Xplore. Restrictions apply.